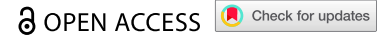


ORIGINAL RESEARCH



HUNK as a key regulator of tumor-associated macrophages in triple negative breast cancer

Nicole Ramos Solis^{a,b}, Anthony Cannon^c, Tinslee Dilday^{a,b}, Melissa Abt^a, Adrian L. Oblak^d, Adam C. Soloff^e, Mark H. Kaplan^{c,b}, and Elizabeth S. Yeh^{a,b}

^aDepartment of Pharmacology and Toxicology, Indiana University School of Medicine Indianapolis, Indianapolis, IN, USA; ^bSimon Comprehensive Cancer Center, Indiana University School of Medicine Indianapolis, Indianapolis, IN, USA; ^cDepartment of Microbiology and Immunology, Indiana University School of Medicine Indianapolis, Indianapolis, IN, USA; ^dDepartment of Radiology and Imaging Sciences, Indiana University School of Medicine Indianapolis, Indianapolis, IN, USA; ^eDepartment of Cardiothoracic Surgery, University of Pittsburgh, Pittsburgh, PA, USA

ABSTRACT

Triple-negative breast cancer (TNBC) lacks the expression of estrogen receptor (ER), progesterone receptor (PR), and human epidermal growth factor receptor 2 (HER2). TNBC tumors are not sensitive to endocrine therapy, and standardized TNBC treatment regimens are lacking. TNBC is a more immunogenic subtype of breast cancer, making it more responsive to immunotherapy intervention. Tumor-associated macrophages (TAMs) constitute one of the most abundant immune cell populations in TNBC tumors and contribute to cancer metastasis. This study examines the role of the protein kinase HUNK in tumor immunity. Gene expression analysis using NanoString's nCounter PanCancer Immune Profiling panel identified that targeting HUNK is associated with changes in the IL-4/IL-4 R cytokine signaling pathway. Experimental analysis shows that HUNK kinase activity regulates IL-4 production in mammary tumor cells, and this regulation is dependent on STAT3. In addition, HUNK-dependent regulation of IL-4 secreted from tumor cells induces polarization of macrophages into an M2-like phenotype associated with TAMs. In return, IL-4 induces cancer metastasis and macrophages to produce epidermal growth factor. These findings delineate a paracrine signaling exchange between tumor cells and TAMs regulated by HUNK and dependent on IL-4/IL-4 R. This highlights the potential of HUNK as a target for reducing TNBC metastasis through modulation of the TAM population.

ARTICLE HISTORY

Received 16 October 2023
Revised 30 May 2024
Accepted 31 May 2024



Keywords


Breast cancer; HUNK; IL-4; tumor associated macrophage

Introduction

Breast cancer is considered one of the most prevalently diagnosed cancers worldwide that primarily affects women.¹ BC is considered a heterogeneous disease, broadly defined based on the expression of hormone receptors including estrogen (ER) and progesterone (PR) receptors, as well as the human epidermal growth factor receptor (HER2). Breast cancer can be further classified into four main subtypes which are Luminal A, Luminal B, HER2-enriched, and triple-negative.¹⁻⁴ Triple-negative breast cancer (TNBC) is a subtype of breast cancer that lacks the expression of estrogen receptors, progesterone receptors, and the aberrant expression of the HER2 receptor.^{3,5} TNBC accounts for 10–20% of all breast cancers and disproportionately affects younger women predominantly of African/African American or multiracial descent.^{3,5} Some clinical characteristics of patients diagnosed with TNBC include poor prognosis, high recurrence, and higher distant metastasis rates.⁶ Due to the tumors lacking hormone receptors and HER2, expression TNBC patients cannot be treated with endocrine therapy or HER2 targeted treatment.^{1,7} Therefore, the standard treatment for TNBC includes chemotherapy or conventional postoperative adjuvant chemoradiotherapy.⁸

More recent studies have focused on characterizing the heterogeneity of TNBC, to explore new treatment alternatives. TNBC exhibits a higher potential for tumor-infiltrated lymphocytes (TILs) within the tumor microenvironment (TME).^{9,10} Apart from TILs, another immune cell that is abundant in the TME and has been shown to contribute to TNBC metastasis is tumor-associated macrophages (TAMs).¹¹⁻¹³ TAMs are described as a heterogeneous cell population that can be polarized in response to signals enriched in the microenvironment in which they are sustained. In both humans and mice, TAMs are broadly classified into either the “classically activated” M1 subtype or the “alternately activated” M2 subtype.¹⁴⁻¹⁶ Markers to identify this population in mice differ from humans. In mice, M1-polarized macrophages are primarily recognized for their antitumoral function and can be characterized by their expression of nitric oxide synthase (iNOS) and support antitumor immunity through the production of superoxide anions and nitrogen-free radicals.^{17,18} However, in humans, M1-polarized macrophages are typically identified by surface markers such as CD86 and CD64.¹⁹ In contrast, M2 TAMs, typically identified by surface markers such as CD206 and Arg1, share similar functions in both species and exhibit pro-tumoral and immunosuppressive

CONTACT Elizabeth S. Yeh  esyeh@iu.edu  Department of Pharmacology and Toxicology, Indiana University School of Medicine Indianapolis, Indianapolis, IN 46202, USA

 Supplemental data for this article can be accessed online at <https://doi.org/10.1080/2162402X.2024.2364382>

© 2024 The Author(s). Published with license by Taylor & Francis Group, LLC.

This is an Open Access article distributed under the terms of the Creative Commons Attribution-NonCommercial License (<http://creativecommons.org/licenses/by-nc/4.0/>), which permits unrestricted non-commercial use, distribution, and reproduction in any medium, provided the original work is properly cited. The terms on which this article has been published allow the posting of the Accepted Manuscript in a repository by the author(s) or with their consent.

functions.²⁰ Polarization and activation of M2 TAMs are mediated primarily by cytokines of a T_H2-type immune response, which includes the production of interleukin 4 and 13 (IL-4 and IL-13) that reprogram macrophage function toward an anti-inflammatory and immune evasive one.^{16–18–21}

Intriguingly, our work and others have shown the relationship between hormonally up-regulated neu-associated kinase (HUNK) and breast cancer progression.^{22–25} HUNK is a serine-threonine protein kinase, a member of the Snf-1/AMPK protein kinase family.²⁶ Some of the described functions of HUNK in cancer include promoting breast cancer metastasis.^{22,25} HUNK was shown to promote metastasis using the MMTV-myc genetically engineered mouse model.²² We also showed that HUNK-dependent phosphorylation of EGFR at threonine (T) 654, resulted in increased metastatic phenotypes in human TNBC breast cancer cells and metastasis *in vivo* using the 4T1 tumor model.²⁵ More recently, our group published work that described that *HUNK* gene alterations correlate with poorer survival outcomes. Using data mined from cBioPortal, we were able to evaluate a subset of breast tumors that had genomic, proteomic, and phospho-proteomic data available. When we looked at the genomic and proteomic data, we found that immune system pathways including chemokine and cytokine signaling were significantly altered in tumors that had *HUNK* gene alterations compared to those that did not, suggesting that HUNK may have a role in breast cancer tumor immunity.²⁷ Chemokines and cytokines are known for their multifunctional role in cancer by affecting immune-cell infiltration and function in the TME, including macrophages, and for their effect on breast cancer growth and metastasis. Therefore, in this study, we aimed to evaluate the role of HUNK in tumor immunity. We provide evidence in this study that HUNK regulates the cytokine IL-4 in cancer cells and modulates the polarization of TAMs. We demonstrate a novel function for HUNK in tumor immunity, highlighting that targeting this kinase is a potential strategy for the modulation of TAMs as an anti-metastatic immunotherapy.

Methods

Cells and culture conditions

All cells were originally obtained from the American Type Culture Collection (ATCC) and maintained in a humidified 5% CO₂ incubator at 37°C. 4T1 cells were maintained in the Roswell Park Memorial Institute Medium (RPMI-1640) (Corning –10–041-CV). RAW 267.4 and EO771 cells were maintained in Dulbecco's modified Eagle's medium (DMEM) (Corning –10–017-CV). All media were supplemented with 10% heat-inactivated Fetal Bovine Serum (FBS) (Gibco, Thermo Fisher Scientific – A5670701), L-Glutamine (Corning – 25–005-CI), and Penicillin Streptomycin solution (Corning – 30–002-CI), unless otherwise specified.

Generation of transduced and transfected cells

4T1 cells and EO771 cells expressing HUNK or K91M were generated as previously described.²⁴ All cell lines with HUNK modifications were maintained in puromycin-containing

media. EO771 selected with 2 µg/ml puromycin. 4T1^{CTL} and 4T1^{HUNK^{sh}} cells were grown in 2 µg/ml puromycin as previously described.²⁵ 4T1 cells were transfected with vector, pcDNA-HA-HUNK, pcDNA-HA-K91M, pcDNA-Stat3 was a gift from Jim Darnell (Plasmid #8706; <http://n2t.net/addgene:8706>; RRID:Addgene_8706; Addgene, Watertown, Massachusetts²⁸) and pcDNA-EGFR.

Pre-made lentiviral particles used to express mouse IL-4 were purchased from Vector Builder (Chicago, Illinois) and were added to 4T1^{HUNK^{sh}} cells per the manufacturer's instructions. After 72 h, transduced cells were visualized by fluorescence microscopy. Transduced cells were selected by using Blasticidin (15ng/ul) (InvivoGen's – ant-bl-05). Cell lines were tested for mycoplasma using MycoFluor™ Mycoplasma Detection Kit (Thermo Scientific – M7006)

Western blotting

Cells were lysed in buffer containing final concentrations of 50 mM Tris-HCl, pH 7.5; 150 mM NaCl; 1% Triton X-100; supplemented with HALT protease and phosphatase inhibitor cocktail (Thermo Scientific, –78440). Primary antibodies used for western blotting are p-EGFR (pT654 – GenTex), EGFR (Santa Cruz – sc-373,746), β-tubulin (Santa Cruz – sc-55,529), p-STAT6 (Thermo Fisher – 700247), STAT6 (Cell Signaling – 5397S), p-STAT3 (Cell Signaling –9145), STAT3 (Cell Signaling – 12640), HUNK (Invitrogen – PA5–28765), Arginase-1 (Santa Cruz – sc-271,430), HA (Cell Signaling – 3724S), IL-4 (Santa Cruz – sc-53,084), IL-4 R alpha (Santa Cruz – sc-28,361), CD206 (Cell Signaling –24595), EGF (Invitrogen – MA5–15606) and F4/80 (BioRad – MCA497). Imaging and quantification were performed on the ChemiDoc imaging system using Image Lab software (BIO-RAD) or the FluorChem-R with AlphaView software (ProteinSimple). To quantify bands, a box was drawn around it, and the signal within the box was quantified. Imaging software reported both the background subtracted volumes (called adjusted volumes) as well as the non-background subtracted volumes (simply called volumes) used for quantification.

RNA isolation and quantitative RealTime PCR

RNA was prepared by using the GeneJet RNA isolation kit (Thermo Scientific – K0732). The synthesis of cDNA from the RNA template was performed using the iScript™ Reverse Transcription Supermix 5X (BioRAD –1708840). The resulting cDNA was used to perform quantitative RealTime PCR using the iTaq™ Universal SYBR Green Supermix (BioRAD –1725120) system. All Primer SYBR Green Assay was purchased from BioRAD; *Hunk* (BioRAD –10025636 qMmuCID0022653), *Stat3* (BioRAD –10025636 qMmuCID0044698), *Egfr* (BioRAD –10025636 qMmuCID0007564), *Il4* (BioRAD –10025636 qMmuCID0006552), *Il13* (BioRAD –10025636 qMmuCED0044968), *Egf* (BioRAD –10025636 qMmuCID0019249). Expression levels of genes were normalized to *Gapdh* Forward: (5'-ATGGTGAAGGTCGGTGTGAACG-3'), Reverse: (5'-CGCTCCTGGAAGATGGTGTATGG-3').

Enzyme-linked immunosorbent assay (ELISA)

For IL-4 cytokine detection, cells were seeded at 1×10^6 cells in a 6 cm tissue culture plate and maintained in serum-free media for 24 h. After 24 h, cell-free media were collected for ELISA. IL-4 concentrations were measured with an IL-4 Mouse ELISA Kit (eBioscience Co – BMS613) and performed per the manufacturer's recommended protocol. A series of cytokine concentrations (0, .63, 1.25, 2.50, 5.0, 10.0, 20.0, 40.0 pg/mL) were used to plot the standard curve. The concentrations within the culture medium collected from different experimental groups were determined by applying the optical density value to the standard curve.

In vitro macrophage polarization assay

To assess M2-polarization markers, Raw 264.7 cells were stimulated with 20 ng/ml of recombinant IL-4 (R&D Systems – 404-ML) for 24 h. To assess M1-polarization markers, cells were stimulated with 10 ng/ml LPS (Novus Biologicals, LLC – NBP2 -25,295) plus 100 IU/ml IFN- γ (R&D Systems –485-MI). After treatment, cells were washed and harvested for downstream application.

To assess macrophage polarization by conditioned media, 4T1 cells (1×10^6 cells) were seeded in 10 cm plates in RPMI1640-free serum medium for 24 h. After 24 h, the supernatants were harvested and filtered through a 0.45 mm membrane and frozen at -80°C until use. Raw 264.7 cells were seeded at a density of 3×10^5 cells/well into a 6-well plate. The following day, media was removed, and cells were washed; 4T1 condition media (CMs) were placed into the six wells plates containing Raw 264.7 cells and incubated in a standard humidified incubator at 37°C in a 5% CO_2 atmosphere for up to 24–48 hours. Cells were then collected and harvested for downstream application. To assess inhibition of polarization Raw 264 cells were treated with a 1:10 dilution of α -IL4 receptor (IL-4 R) antibody for 15 min, followed by IL-4 (Santa Cruz Biotechnology – sc-28,361).

Isolation, culture, and differentiation of bone marrow-derived cells

Bone marrow was isolated from 6–8-week-old female BALB/c and BALB/c-*IL4ra*^{tm1Sz/J} mice as described.²⁹ The left femora and tibiae were removed from the surrounding soft tissues. Both ends of the bone were resected with a bone cutter, and bone marrow cells were collected by flushing the diaphysis of each bone with isolation media (PBS supplemented with 1% FBS) using a 5-ml syringe fitted with a 20-gauge needle. Bone marrow cells isolated from femora or tibiae in each animal were combined. Cells were dispersed by repeatedly pipetting the cell suspension using a 10-ml syringe fitted with a 22-gauge needle and filtering through a 70- μm filter mesh. Single-cell suspensions were obtained, and red blood cells were removed by 1:1 dilution of RBCO Lysis Buffer (Invitrogen –00-4333-57). The reaction was stopped by adding 1X PBS, cells were collected by centrifugation and resuspended in PBS. Cells were cultured with alpha-modified MEM supplemented with 10% FBS and Penicillin Streptomycin solution overnight.

For monocyte differentiation, 20 ng/ml of M-CSF (Cell Signaling Technology –5228) was added to the complete medium. Cells were cultured, and media was replaced every 3 d. After 7 d of culture with M-CSF, macrophages were identified using CD11b (Novus –NB110-89474SS) western blotting or analysis by flow cytometry.

NanoString analysis

The NanoString's nCounter PanCancer Immune Profiling panel (NanoString Technologies™, Seattle, Washington, USA) is composed of >700 tumor immune specific genes used for gene expression profiling on the nCounter platform (Nanostring, Seattle, WA) as described by the manufacturer. NanoString nSolver 4.0 software was used for the analysis of gene expression values. Quality control, background correction, and data normalization were performed according to NanoString Gene Expression Data Analysis Guidelines. Data can be accessed via NCBI GEO (GSE242859).

Animal care

Animal care and experiments were approved and executed under the guidelines of the Indiana University School of Medicine IACUC. All animals were housed and cared for in the AAALAC-accredited Animal Research Center at the Indiana University School of Medicine and routinely monitored by laboratory personnel and veterinary staff. Animals were euthanized by isoflurane overdose per the Guide for the Care and Use of Laboratory Animals. Protocols were in place for early and humane endpoints if an experimental animal displayed signs of illness. Tumor measurements and health monitoring were performed regularly by lab and veterinary staff.

Orthotopic tumor models and IL-4 treatment

Mice were acquired from Jackson Labs (Strain #: 000651). To generate tumors, female BALB/c mice were anesthetized using a mix of isoflurane and oxygen. 4T1 cells were resuspended in regular media and then injected into the abdominal mammary gland at 50,000 cells per gland. Once the tumors reached a volume of ($\sim 1000 \text{ mm}^3$) (approximately 3 weeks post injection), they were isolated. Tumors were digested for the generation of single-cell suspensions, which was performed by using a Mouse Tumor Dissociation Kit (Miltenyi Biotec –130-096-73). Tumor and red blood cells were excluded using a ficoll gradient, and the remaining cells were used for downstream applications including RNA isolation, flow cytometry, and western blot. For IL-4 treatment, female BALB/c and BALB/*IL4ra*^{tm1Sz/J} mice were injected as described above and tumors were generated. After 1-week post-injection, treatment of IL-4 started; mice were intraperitoneally treated with vehicle (PBS) or recombinant IL-4 (10 $\mu\text{g}/\text{kg}$) (Pepro Tech, NJ, 214–14) every other day for 1 week. After the end of treatment (on day 14) mice were placed under observation for 5 d and sacrificed following IACUC guidelines, and tumors and lungs were collected. Metastasis for each experiment was evaluated by isolating and sectioning of the lung followed by H&E staining to

visualize lung metastasis. Total metastatic lesions per lung were counted. For both experiments, tumor growth was monitored every 3 d, and tumor volume was calculated.

Tumor-associated macrophages isolation

The tumors were minced with razor blades and digested for the generation of a single-cell suspension as described above. Isolation of TAMs was performed by immunomagnetic negative selection using EasySep™ Mouse Monocyte Isolation Kit (STEMCELL Technologies -19,761).

Flow cytometry

Fixable Viability Stain 620 (BD Biosciences) was used to discriminate between live and dead cells. The cells were then blocked with Fc-block (BD Biosciences) permeabilized and stained with antibodies for 30 min in the dark at 4°C. Antibodies are anti-mouse F4/80 (Biolegend – B209472), anti-mouse Arginase-1 (Invitrogen 53-3697-80), anti-mouse CD45 (Biolegend –103149), viability dye (Invitrogen – 65-0865-14), and anti-mouse CD206 (Biolegend – 141708). Stained samples were analyzed on a Cyan ADP 9 color cytometer (Beckman Coulter), and analysis was performed with FlowJo software version 10. Each fluorochrome was compensated against all the other fluorochromes. As internal controls, we used isotype antibody controls and Fluorescence Minus One (FMO) control to verify the specificity of the signal for each cell surface marker. About 5–10,000 events of the smallest population were acquired, to ensure statistical power for the analysis.

Measurement of IL-4 in serum

Once the tumors reached a volume of (~1000 mm³), mice were euthanized, and blood was drawn by cardiac puncture. Collected whole blood was placed in a microcentrifuge tube. The blood was allowed to clot by leaving it undisturbed at room temperature for 15–30 min. The blood clot was removed by centrifuging at 1,000–2,000 × g for 10 min at 4°C. Following centrifugation, the serum was used to measure IL-4 levels by an ELISA kit (BioLegend's ELISA Max™ –431101). ELISA was performed by following the manufacturer protocol.

Statistical analysis

Group measurements comparing two groups were compared using a two-tailed Student's t-distribution. Error bars represent the standard error of the mean. Data are representative of at least three independent experiments with at least three individual replicates or more per experiment. One-way ANOVA with Tukey's multiple comparisons was used to compare the means of three or more groups. *p* values were calculated using GraphPad Prism software. *, *p* < 0.05; **, *p* < 0.01; ***, *p* < 0.001, ****, *p* < 0.0001. Metastases in the lungs were analyzed using a blind study analysis. The total number of metastatic lesions was counted per lung and used to generate group averages, which were compared between groups and analyzed by T-test (for two samples) or one-way ANOVA (for three or more samples). Tumor growth curves were analyzed using

two-way ANOVA with Tukey's multiple comparisons. The figures in this manuscript were created with BioRender.com and Adobe Illustrator. Graphics and Statistical analysis were performed using GraphPad Prism (version 7 & 8).

Results

HUNK has a potential role in regulating tumor immunity

Although a role for HUNK in breast cancer metastasis has previously been reported,²⁵ a role for HUNK in tumor immunity has not been described. To explore the effect of HUNK in tumor cells on the immune compartment within the TME, we performed a gene expression analysis using NanoString's nCounter PanCancer Immune Profiling panel, which contains >700 tumor immune-specific genes and allowed us to specifically target our analysis to immune profiling. To generate tumors, we modified HUNK in the epithelial 4T1 tumor cells and generated control (CTL) or HUNK knockdown (shRNA) cell lines (Figure 1(a)). We isolated tumors from mice orthotopically implanted with 4T1^{CTL} and 4T1^{HUNKsh} cells. HUNK knockdown in the tumors was confirmed by quantitative RealTime PCR (Figure 1(b)). We also confirmed our previously reported findings²⁵ that tumor growth was not affected (Figure 1(c)), and mice with tumors derived from 4T1^{HUNKsh} cells had reduced levels of lung metastasis compared to 4T1^{CTL} tumors (Figure 1(d)). nCounter analysis was performed on *n* = 3 biological replicates from 4T1^{CTL} and 4T1^{HUNKshA} tumors which showed tight clustering of gene expression within tumor groups. We identified ~100 mRNA targets that were significantly altered in HUNK-depleted (4T1^{HUNKshA}) tumors (Figure 1(e)) and further analyzed the significantly altered mRNA targets using Reactome pathway analysis tool. Based on the set of mRNA targets that were significantly altered in the HUNK-depleted group, the Reactome pathway analysis indicated that IL-4 and IL-13 cytokine signaling, which acts through the IL-4 receptor (IL-4 R), was significantly decreased (Figure 1(e)). To validate these findings, we measured *Il4* and *Il13* expression levels in 4T1^{CTL} and 4T1^{HUNKsh} tumors by RealTime PCR. Results show that 4T1^{HUNKsh} tumors had reduced *Il4* gene and protein expression levels (Figure 1(f–g)); however, no significant changes were observed in *Il13* (Supplementary Figure S1A) when 4T1^{HUNKsh} tumors were compared to 4T1^{CTL} tumors.

HUNK regulates IL-4 production in 4T1 cells

Because we originally modified HUNK in the epithelial 4T1 tumor cells, we explored tumor cell-intrinsic effects. Secondary confirmation of HUNK depletion in 4T1 cells using two independent shRNAs was performed by RealTime PCR (Figure 2(a)). We then compared IL-4 protein by western blot and *Il4* expression in 4T1^{CTL} and 4T1^{HUNKsh} cells by RealTime PCR. We found that 4T1^{HUNKsh} expressing cells had lower levels of both IL-4 protein (Figure 2(b)) and *Il4* mRNA compared with 4T1^{CTL} cells (Figure 2(c)). We also measured *Il13* expression and results correlated with observations in tumors where no statistically significant changes were observed in *Il13* levels between 4T1^{CTL} and 4T1^{HUNKsh} cells

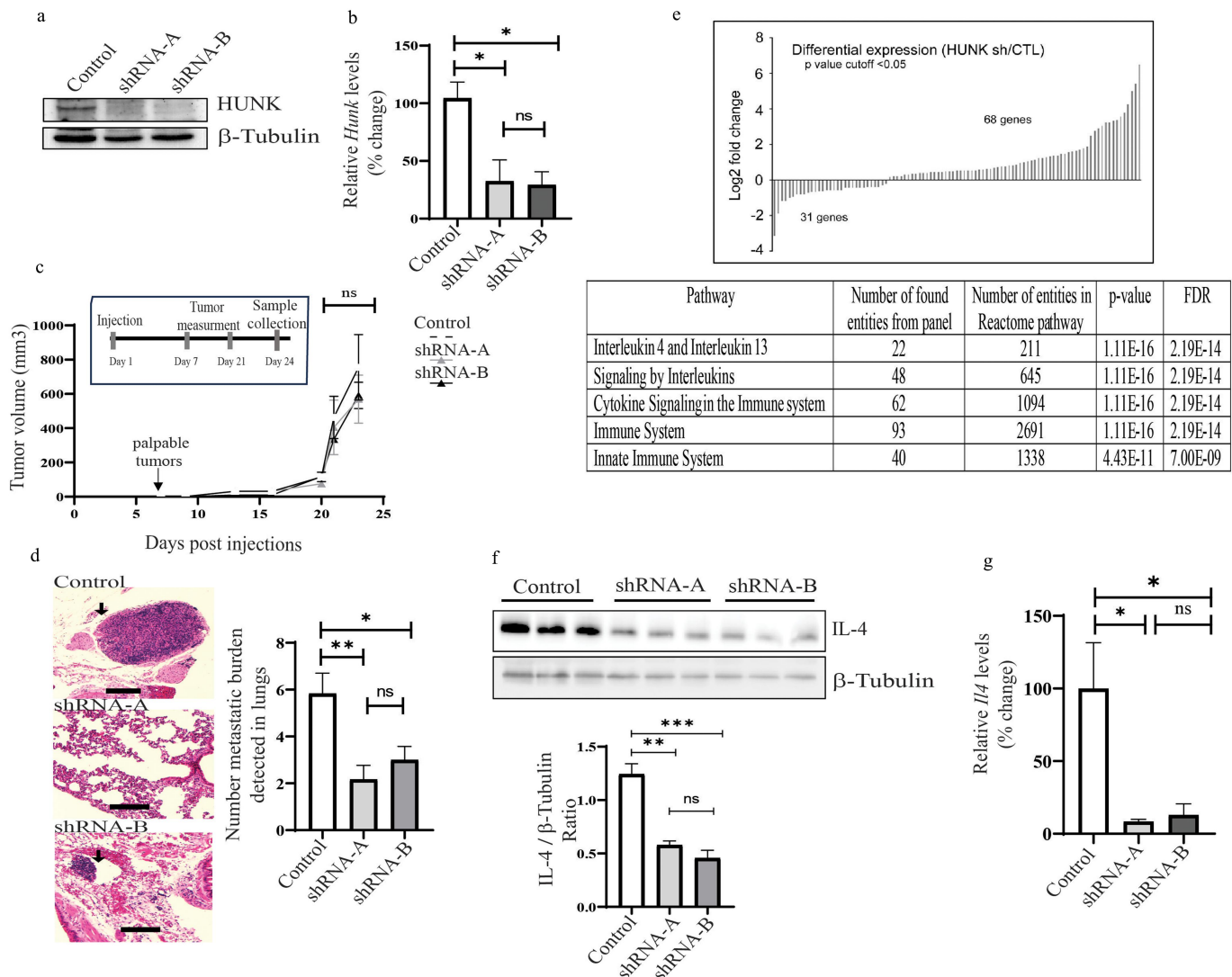


Figure 1. HUNK regulates TNBC tumor immunity. **A.** Western blot analysis for HUNK in 4T1^{CTL} and 4T1^{HUNKsh} cells. **B.** *Hunk* mRNA levels from 4T1^{CTL} and 4T1^{HUNKsh} tumors were analyzed by RealTime PCR. **C.** Tumor growth was assessed by measuring tumor length and width; tumor growth was not affected. **D.** Lungs isolated from both 4T1^{CTL} and 4T1^{HUNKsh} orthotopic model were analyzed for tumor burden by H&E. The quantification of tumor burden on the lung is represented in column graph where 4T1^{HUNKsh} lungs exhibited reduced levels of metastasis compared to 4T1^{CTL} lungs. **E.** 4T1^{CTL} and 4T1^{HUNKsh} (shA) orthotopic mammary tumors were used to assess NanoString's nCounter PanCancer Immune Profiling panel. A total of 99 mRNA targets were significantly altered in HUNK-depleted tumors. Significantly altered mRNA was analyzed using Reactome pathway analysis tool. Quality control, background correction, and data normalization were performed according to NanoString Gene Expression Data Analysis Guidelines using the nSolver v4.0 software. **F.** Western blot analysis for IL-4 in 4T1^{CTL} and 4T1^{HUNKsh} tumors. **G.** *Il4* mRNA levels from 4T1^{CTL} and 4T1^{HUNKsh} tumors were analyzed by RealTime PCR. For all panels except E, one-way ANOVA was used to compare the mean of three or more groups. $N \geq 3$ tumors per group for all analyses. Data are expressed as mean \pm SEM. *, $p < 0.05$; **, $p < 0.01$; ***, $p < 0.001$.

(Supplementary Figure S1B). We next measured IL-4 secretion by ELISA. The IL-4 protein was detectable in the condition media (CM) isolated from 4T1^{CTL} and 4T1^{HUNKsh} cells after 24 h of cell growth. Results from three independent studies showed that high IL-4 protein levels were found in the CM from 4T1^{CTL} cells but were reduced in 4T1^{HUNKsh} cells (Figure 2d), suggesting that HUNK depletion results in loss of IL-4 secretion.

To determine if HUNK kinase activity is required for *Il4* synthesis and IL-4 secretion, we re-expressed HUNK WT and a kinase-inactive HUNK (K91M) into our 4T1^{HUNKsh} cells (Figure 2e). We found that the addition of HUNK WT into 4T1^{HUNKsh} cells rescued *Il4* expression levels (Figure 2f) and IL-4 secretion (Figure 2g). However, re-expressing HUNK K91M did not (Figure 2f,g). Furthermore, we also saw similar

effects in EO771 cells, where EO771 cells overexpressing HUNK WT showed higher levels of both *Il4* mRNA when compared with EO771 cells expressing HUNK K91M (Supplementary Figure S2).

EGFR is not required for IL-4 production downstream of HUNK in 4T1 cells

We previously identified EGFR as a substrate of HUNK and showed that HUNK phosphorylates this receptor at threonine (T) 654.²⁵ We also found that increased phosphorylation of T654 EGFR in TNBC tumor cells correlates with increased epithelial-to-mesenchymal transition (EMT), migration and invasion, and metastasis.²⁵ A common downstream signaling pathway that is activated by the phosphorylation of EGFR is

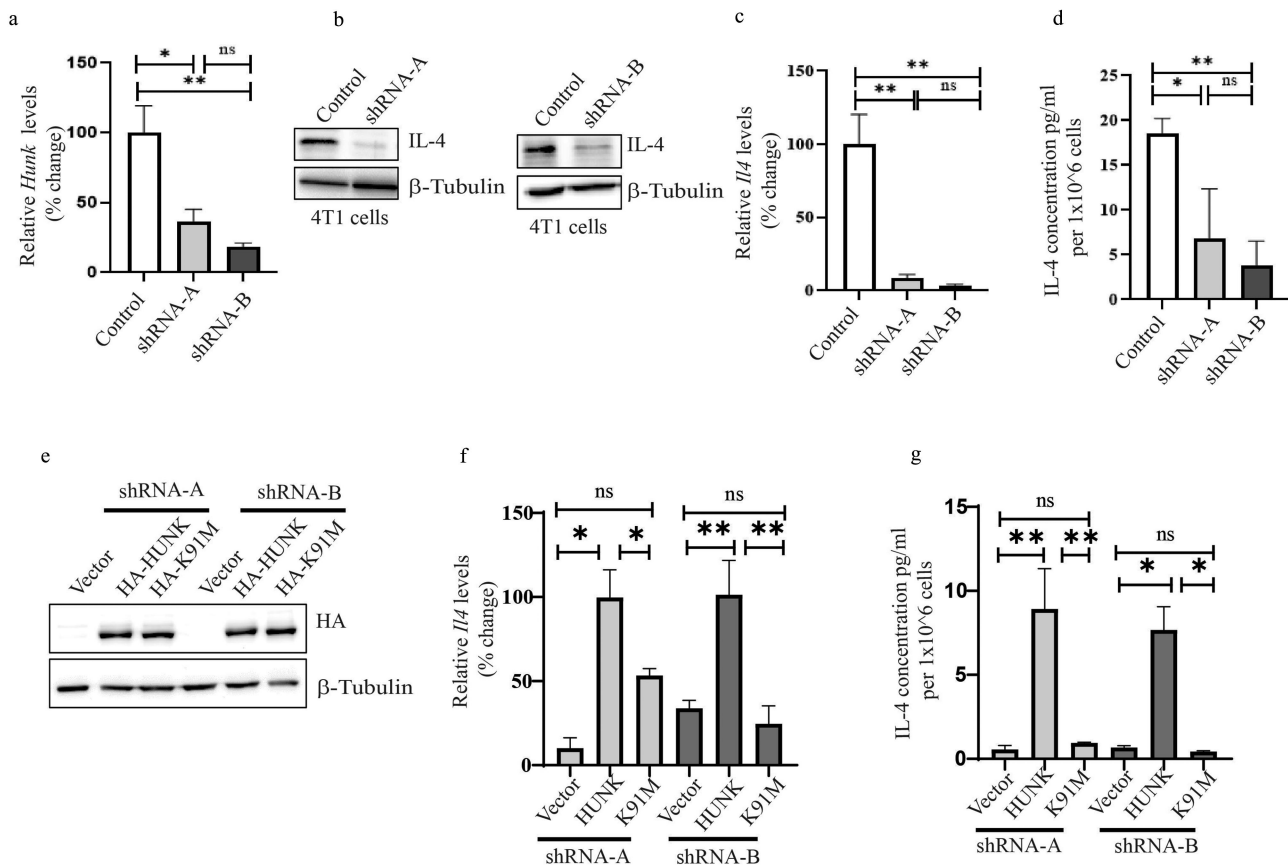


Figure 2. HUNK regulates *Il4* expression and IL-4 secretion in TNBC cells. A. Quantification of *Hunk* mRNA levels on 4T1^{CTL} and 4T1^{HUNKsh} cells. B. Western blot analysis for IL-4 in 4T1^{CTL} and 4T1^{HUNKsh} cells (shA-left, shB-right). C. Quantification of *Il4* mRNA levels on 4T1^{CTL} and 4T1^{HUNKsh} cells. D. IL-4 concentrations in condition media (CM) of 4T1^{CTL} and 4T1^{HUNKsh} cells. ELISA was used to determine the concentration of target protein in each sample by standard curve. E. 4T1^{HUNKsh} cells were transfected with vector, pcDNA-HA-HUNK, or pcDNA-HA-K91M HUNK. Western blots showing re-expression of HA-HUNK and HA-K91M HUNK in 4T1^{HUNKshA} and 4T1^{HUNKshB} cells. F. RealTime PCR analysis of *Il4* levels in 4T1^{HUNKshA} and 4T1^{HUNKshB} cells re-expressing HUNK and K91M. G. IL-4 concentrations measured by ELISA in condition media of 4T1^{HUNKshA} and 4T1^{HUNKshB} cells re-expressing HUNK and K91M. One-way ANOVA was used to compare the mean of three or more groups. Data are expressed as mean \pm SEM of three independent experiments. *, $P < 0.05$; **, $P < 0.01$.

the mitogen-activated protein kinase (MAPKs) pathway (Ras-MAPK-ERK1/2 pathway).^{30,31} Ras-MAPK-ERK downstream signaling pathways have been implicated in the regulation of IL-4 signaling.^{32,33} Therefore, we tested whether the overexpression of EGFR in HUNK knockdown 4T1 cells resulted in the rescue of IL-4 expression but did not see any effect of EGFR on this process (Supplementary Figure S3).

HUNK regulates IL-4 production in a STAT3-dependent fashion

It has also been reported in other cancer models that STAT3 phosphorylation at the tyrosine (Y) 705 site leads to IL-4 transcription.³⁴ Therefore, to elucidate whether STAT3 activation is involved in regulating IL-4 production downstream of HUNK in 4T1 cells, we measured STAT3 phosphorylation at Y705 in 4T1^{CTL} and 4T1^{HUNKsh} cells using western blot. Results showed that phosphorylation of STAT 3 was reduced in 4T1^{HUNKsh} cells (Figure 3a) (shA) & Figure 3b) (shB)).

To determine if HUNK kinase activity affects the phosphorylation of STAT3, we re-expressed HUNK WT and HUNK K91M into our 4T1^{HUNKsh} cells and measured STAT3 phosphorylation. Results showed that the addition of HUNK WT into 4T1^{HUNKshA} and 4T1^{HUNKshB} cells rescued STAT3

phosphorylation but re-expressing K91M did not (Figure 3c) (shA) & Figure 3d) (shB)). To elucidate whether STAT3 activation is required for IL-4 production in 4T1 cells, we overexpressed STAT3 WT in 4T1^{HUNKsh} cells (Figure 3e) (shA) & Figure 3h) (shB)) and measured *Il4* expression levels. The result showed that overexpression of STAT3 in 4T1^{HUNKsh} cells rescued STAT3 phosphorylation (Figure 3f) (shA) & Figure 3i) (shB)) and *Il4* expression (Figure 3g) (shA) & Figure 3j) (shB)). Finally, to elucidate if the rescue of STAT3 phosphorylation recovered the IL-4 secretion in 4T1^{HUNKsh} cells, we measured IL-4 in CM from in 4T1^{HUNKsh} overexpressing of STAT3. The results showed that the overexpression of STAT3 in 4T1^{HUNKsh} cells rescued IL-4 secretion (Figure 3k) (shA) & Figure 3l) (shB)).

HUNK regulation of IL-4 in 4T1 cells induces macrophage polarization

Our data show that IL-4 secretion from 4T1 cells is being regulated by HUNK, and it is well established in the literature that IL-4 is a major activator of TAMs.^{21,35} Therefore, we wanted to assess whether a loss of IL-4 secretion from 4T1 cells due to HUNK-depletion affected macrophage polarization. We designed an *in vitro* approach to assess polarization

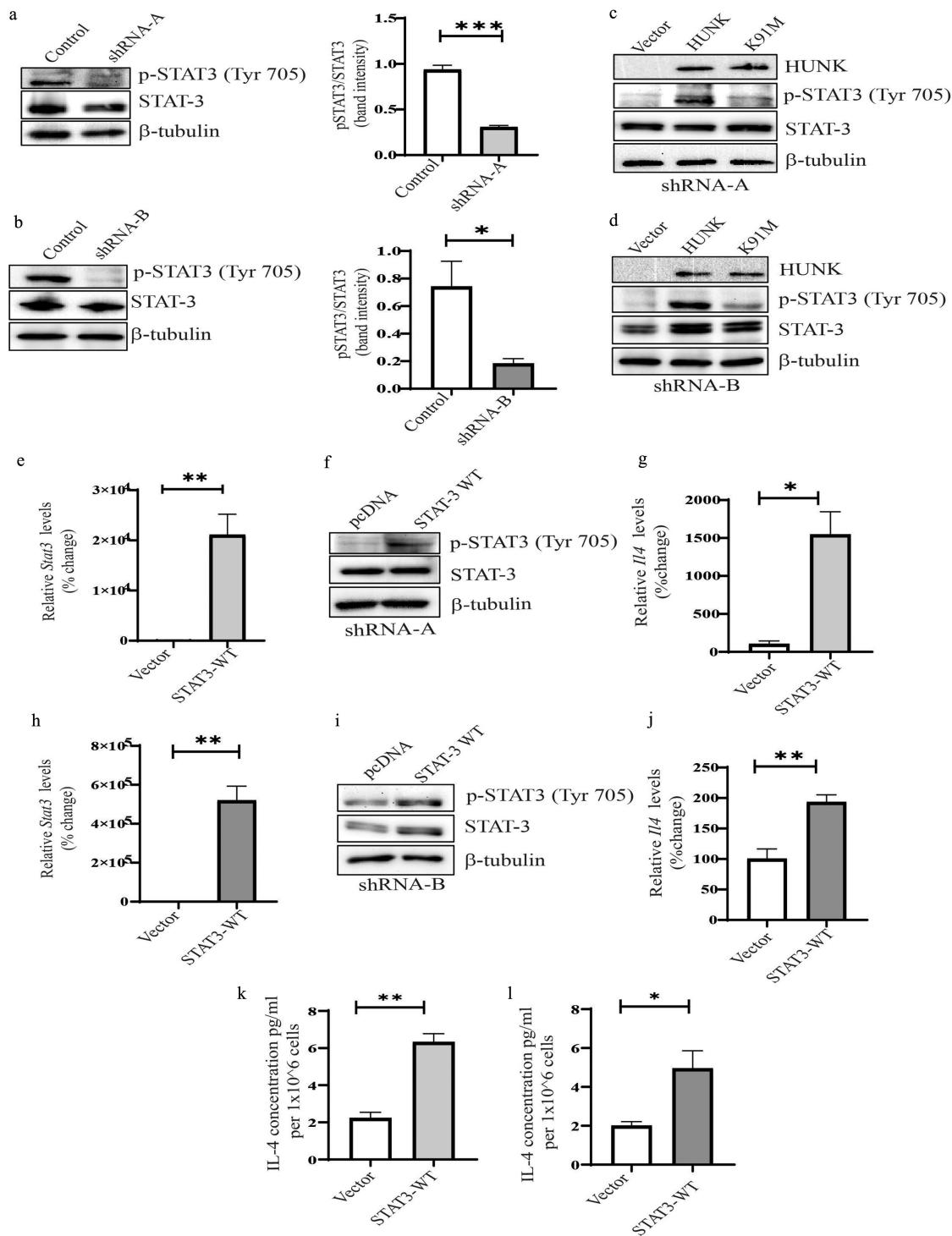


Figure 3. HUNK regulation of IL-4 in cancer cells is dependent on STAT3 activation. A-B. Western blot analysis showing phosphorylation of Stat3 in 4T1^{CTL} and 4T1^{HUNKsh} cells (shA-panel A, shB-panel B). Densitometry shows that the phosphorylation of Stat3 is diminished in 4T1^{HUNKsh} cells. C-D. 4T1^{HUNKshA} and 4T1^{HUNKshB} cells were transfected with vector, pcDNA-HA-HUNK, or pcDNA-HA-K91M. Western blots showing re-expression of HA-HUNK and HA-K91M HUNK in 4T1^{HUNKsh} cells (shA-panel C, shB-panel D). Re-expression of HUNK in 4T1^{HUNKsh} cells rescues phosphorylation of Stat3. E & H. 4T1^{HUNKsh} cells were transfected with vector or pcDNA-Stat3. *Stat3* mRNA levels in 4T1^{HUNKsh} overexpressing Stat3 wild type (WT) were analyzed by RealTime PCR. (shA-panel E, shB-panel H) F & I. Overexpression of Stat3 wildtype in 4T1^{HUNKsh} cells was confirmed by western blotting of total and activated (phosphorylation at Y705) of Stat3. (shA-panel F, shB-panel I) G & J. *Il4* mRNA levels were measured in 4T1^{HUNKsh} overexpressing Stat3. Overexpression of Stat3 in 4T1^{HUNKsh} rescued *Il4* levels. (shA-panel G, shB-panel J) K & L. IL-4 concentrations measured by ELISA in condition media (CM) of 4T1^{HUNKsh} cells overexpressing Stat3. (shA-panel K, shB-panel L). Unpaired t-tests were used to compare the means of two groups. One-way ANOVA was used to compare the mean of three or more groups. Data are expressed as mean \pm SEM of three independent experiments. *, $p < 0.05$; **, $p < 0.01$; ***, $p < 0.001$.

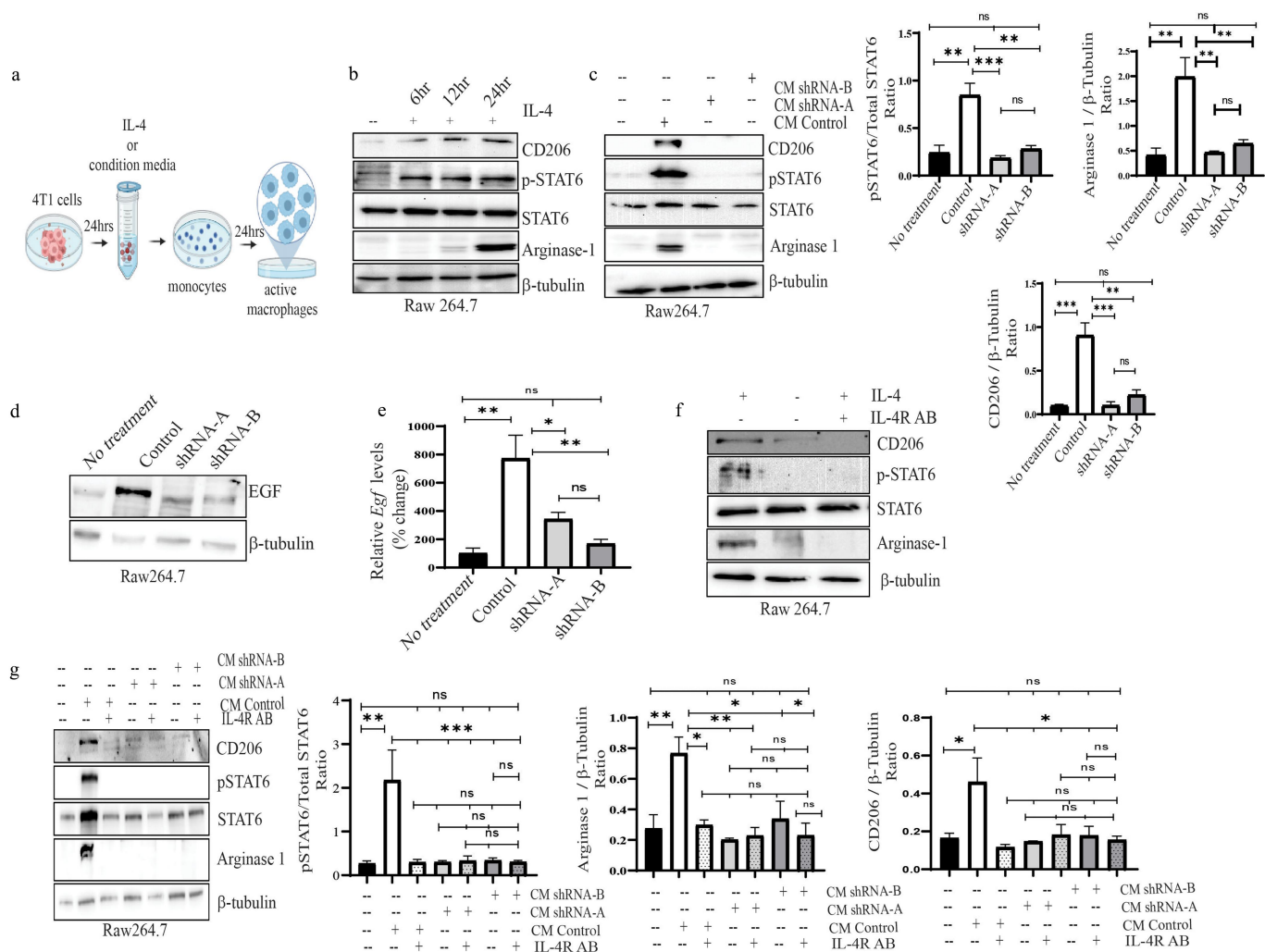


Figure 4. HUNK regulation of IL-4 in 4T1 cells promotes M2 macrophage polarization. A. Experimental schematic. B. Raw 264.7 was treated with 20 ng/ml IL-4. M2 polarization was measured by western blotting for increased expression of CD206, Arginase-1, and Y705 phosphorylation of Stat6. C. Raw 264.7 treated with condition media (CM) from 4T1^{CTL} and 4T1^{HUNKsh} cells. CM-derived from 4T1^{CTL} resulted in M2 polarization measured by western blotting for CD206, Arginase-1, and Y705 phosphorylation of Stat6. Densitometry shows that CM derived from 4T1^{HUNKshA} and 4T1^{HUNKshB} cells do not result in M2 polarization D. Western blot analysis showing Egf expression in Raw 264.7 treated with CM from 4T1^{CTL} and 4T1^{HUNKsh} cells. E. *Egf* expression levels measured by RealTime PCR in Raw 264.7 treated with CM from 4T1^{CTL} and 4T1^{HUNKsh} cells. F-G. Raw 264.7 cells were treated with a 1:10 dilution of a-IL4 receptor (IL-4 R) antibody for 15 min, followed by IL-4 (F) or CM from 4T1^{CTL} and 4T1^{HUNKsh} cells (G). Polarization was assessed by measuring CD206, Arginase 1, and Y705 phosphorylation of Stat6 by western blot. Each experiment was repeated three times. Densitometry shows that Raw 264.7 cells treated with anti-IL4 receptor (IL-4 R) antibody followed by CM derived from 4T1^{HUNKsh} cells do not result in M2 polarization. One-way ANOVA was used to compare the mean of three or more groups. Data are expressed as mean \pm SEM of three independent experiments. *, $p < 0.05$; **, $p < 0.01$; ***, $p < 0.001$.

using the RAW 264.7 cell line (Figure 4a). IL-4 induces activation of macrophages and TAMs primarily by activating IL-4 receptor (IL-4 R) signaling through the Janus kinase/signal transducer and activator of transcription (JAK/STAT) cascades, resulting in STAT6 phosphorylation.³⁶ To analyze *in vitro* polarization by IL-4 in these cells, we first performed a control experiment where recombinant IL-4 was applied to RAW 264.7 cells and IL-4 R signaling was measured by western blot of STAT6 phosphorylation, Arginase 1, and CD206 expression as phenotypical markers.³⁷ Our findings show that IL-4 induced STAT6 phosphorylation, Arginase 1, and CD206 expression (Figure 4b). We next used this *in vitro* approach to ask whether applying CM from our 4T1 cell lines onto the RAW 264.7 cells had a similar effect. Our results show that CM from 4T1^{CTL} induced and increased expression of CD206, Arginase 1, and phosphorylation of STAT-6 in RAW 264.7 but CM from 4T1^{HUNKsh} cells did not (Figure 4c). This

finding is consistent with our earlier experiments showing that 4T1^{HUNKsh} cells have reduced IL-4 production compared to 4T1^{CTL} cells.

Activation of TAMs induced by IL-4 has been reported to increase the induction of epidermal growth factor (Egf) expression from the macrophages, resulting in a paracrine loop that contributes to cancer metastasis.^{38,39} Egf secreted by TAMs promotes a synergistic effect between TAMs and breast cancer cells, promoting cell migration.^{38,39} Consequently, we measured both protein and *Egf* mRNA expression levels in RAW 264.7 treated with CM from both 4T1^{CTL} and 4T1^{HUNKsh} cells. Results showed that RAW 264.7 treated with CM from 4T1^{CTL} have relatively high protein and high *Egf* expression levels compared to cells treated with CM from 4T1^{HUNKsh} (Figure 4d-e). To assess whether IL-4 is directly inducing this polarization on the target cells through IL-4 R, we used an IL-4 R blocking

antibody and showed in a control experiment that IL-4 R antibody blocked STAT6 phosphorylation, CD206, and Arginase 1 after IL-4 treatment (Figure 4f). We then did an experiment where the IL-4 R antibody was applied to block IL-4 R on the target RAW 264.7 cells before adding CM from either 4T1^{CTL} or 4T1^{HUNKsh} cells. Results show that when RAW 264.7 is treated with IL-4 R antibody, CM from 4T1^{CTL} does not induce STAT6 phosphorylation, CD206, or Arginase 1 (Figure 4g), compare lane 2 to lane 3), and as expected from Figure 3(c), CM from 4T1^{HUNKsh} cells does not induce these factors regardless of IL-4 R blocking.

Targeting HUNK modulates the TAM population in the tumor microenvironment

To assess if targeting HUNK influences macrophages *in vivo* in the breast cancer TME, we utilized an orthotopic mammary tumor model. To generate tumors, we implanted 4T1^{CTL} and the two different 4T1^{HUNKsh} cell lines into the mammary gland of BALB/c female mice.

After the tumors reached 10 mm in diameter (day 24 post-injection), they were isolated and analyzed for TAMs by flow cytometry. Cellular markers used to identify this cell population in tumors were CD45⁺ (hematopoietic cells), F4/80⁺ (macrophages), CD206⁺, and ARG1⁺ (M2 macrophage subpopulation) (Figure 5a). Results show that tumors derived from 4T1^{HUNKsh} cells have lower percentages of CD206⁺ and double positive CD206 and Arginase 1, CD45/F480⁺ cells, compared to tumors derived from 4T1^{CTL} cells (Figures 5b,c). Gating strategies for flow cytometry analysis are shown in Supplementary Figure S4.

It has been reported that IL-4 plays a significant role in inducing TAM polarization and regulating their pro-tumoral and metastatic potential.⁴⁰ IL-4 released from tumor cells stimulates IL-4 R on TAMs, leading to *Egf* expression and further *Il4* expression from the TAMs.^{41,42} *Egf* released from TAMs can promote cancer metastasis by signaling to EGFR on tumor cells, creating a paracrine signaling loop between TAMs and tumor cells.⁴³ We first measured IL-4 levels in the serum from mice by ELISA (Figure 5d) but we did not see any effect of HUNK in

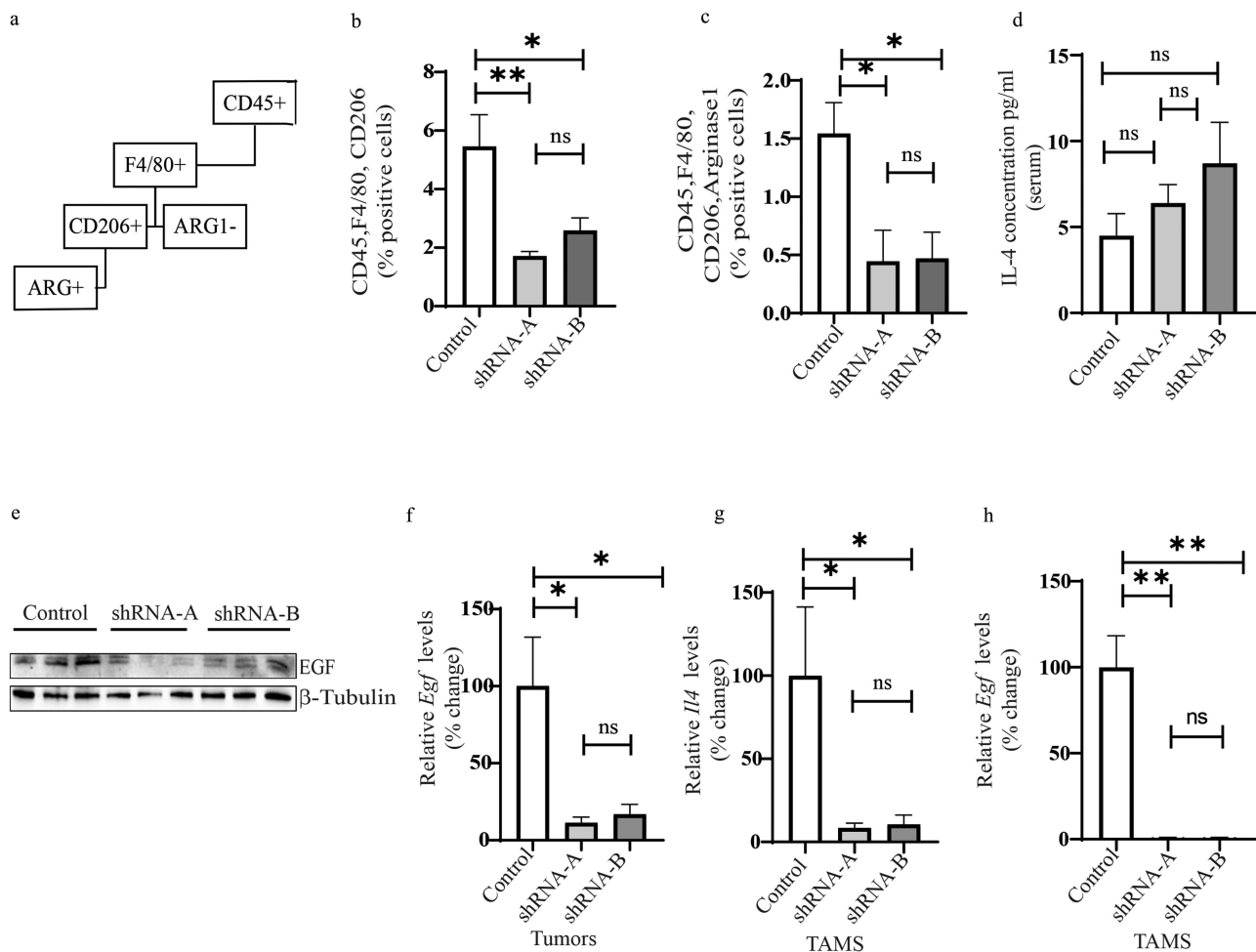


Figure 5. Targeting HUNK modulates the TAM population in tumors. A. Representation of flow cytometric gating strategy and analysis of markers used to identify M2 macrophages present in tumors. B-C. Percentage of positive CD206 cells (subset from CD45⁺/F4/80⁺ cells) on tumors derived from 4T1^{CTL} and 4T1^{HUNKsh}. Further analysis of TAMs from 4T1^{CTL} and 4T1^{HUNKsh} tumors was performed by quantification of percentages of Arginase 1 positive cells (subset from CD45⁺/F4/80⁺/CD206⁺ cells). D. IL-4 concentrations in serum of mice with 4T1^{CTL} and 4T1^{HUNKsh} tumors. ELISA was used to determine the concentration of target protein in each sample by standard curve. E. Western blot showing *Egf* levels from 4T1^{CTL} and 4T1^{HUNKsh} tumors. F. RealTime PCR analysis of *Egf* levels from 4T1^{CTL} and 4T1^{HUNKsh} tumors. G-H. TAMs were isolated from 4T1^{CTL} and 4T1^{HUNKsh} tumors. Expression of *Il-4* and *Egf* levels was measured by RealTime PCR. Statistical analyses were performed using one-way ANOVA. Data are expressed as mean \pm SEM. *, $P < 0.05$; **, $P < 0.01$; ***, $P < 0.001$.

systemic IL-4 regulation in the host. Next, we analyzed *Egf* expression and *Egf* protein levels in the tumors. Results showed that tumors derived from 4T1^{HUNKsh} cells have reduced protein (Figure 5e) and mRNA levels of *Egf* (Figure 5f) compared to control cells. *Il4* levels in 4T1^{CTL} and 4T1^{HUNKsh} tumors were previously shown in Figure 1g). IL-4 R activation on TAMs by IL-4 leads to the production of *Egf* and more IL-4. Therefore, we also evaluated *Egf* and *Il4* in the TAMs isolated from tumors. Consistent with our findings and the concept of a paracrine signaling loop between tumor cells and TAMs, we saw that TAMs isolated from 4T1^{HUNKsh} tumors also have low *Il4* levels (Figure 5g) and *Egf* levels (Figure 5h) compared with TAMs from 4T1^{CTL} tumors. Our findings suggest a model that HUNK-dependent IL-4 released from tumor cells leads to activation of IL-4 R on TAMs, which in turn causes TAMs to produce more IL-4 and *Egf*. Consequently, inhibiting HUNK impairs IL-4 regulation in 4T1 cells, resulting in a low availability of IL-4 in the TME. Therefore, there would be less exposure of TAMs to IL-4 in the TME, leading them to lose further production of IL-4 and production of *Egf*, breaking the paracrine loop between tumor cells and TAMs (Supplementary Figure S6).

Macrophage polarization by HUNK is dependent on the IL-4/IL-4 R paracrine interaction

Our results show that blocking IL-4-to-IL-4 R signaling on macrophages *in vitro* impairs M2 polarization. To further explore this observation, we made use of the homozygous IL-4 R knockout (BALB/c-*Il4ra*^{tm1Sz/J}), herein referred to as *Il4r*^{-/-} mice (Supplementary Figure S5A). *Il4r*^{-/-} mice exhibit a loss of IL-4 R expression and signal transduction and are an essential tool for studying the role of IL-4/IL-4 R-directed immunological pathways.⁴⁴ To further assess our findings, we first isolated bone marrow cells from *Il4r*^{-/-} and BALB/c wild type (*wt*) mice and differentiated these cells into macrophages, confirmed by western blot for the macrophage marker F4/80 (Supplementary Figure S5B) and flow cytometric quantitation of the CD45⁺/F4/80⁺ cell population (Supplementary Figure S5C,D). After 5 d of differentiation, we analyzed the purity of the cell subpopulations by flow cytometry using CD45 (hematopoietic cells), and F4/80 (macrophages) as markers (Supplementary Figure S5C). Results showed that after differentiation we obtained a yield of >80% CD45/F4/80 double-positive cells in both the *wt* and *Il4r*^{-/-} mouse model and, therefore, we concluded that differentiation of bone marrow-derived macrophages is not impaired in the *Il4r*^{-/-} mice (Supplementary Figure S5D). Next, we polarized bone marrow-derived macrophages (BMDM) into an M2 subpopulation. Results showed that BMDM from BALB/c *wt* mice had increased phosphorylation of STAT6, suggesting M2 polarization, however, BMDM derived from *Il4r*^{-/-} mice did not (Supplementary Figure S5E). We also characterized these cells by flow cytometry using CD45 (hematopoietic cells), F4/80 (macrophages), Cd11b, and CD206 (M2) as markers (Supplementary Figure S5F). The flow cytometry analysis

showed that the total subpopulation of BMDM that is M2 is significantly higher from BALB/c *wt* mice after polarization by IL-4, whereas the subpopulation of M2 from BMDM of *Il4r*^{-/-} mice is less than 1% after IL-4 stimulation (Supplementary Figure S5G).

Overexpression of IL-4 in 4T1^{HUNKsh} cells rescues phosphorylation of Stat6 in macrophages and metastasis

Thus far, our results show that 4T1^{HUNKsh} cells have low levels of IL-4 protein secretion and *Il4* mRNA expression. We also show that CM isolated from 4T1^{HUNKsh} does not induce macrophage polarization *in vitro* and tumors derived from 4T1^{HUNKsh} have lower numbers of TAMs in the TME compared to 4T1^{CTL} tumors. To test whether the overexpression of IL-4 in 4T1^{HUNKsh} cells will rescue macrophage polarization toward M2 phenotypes, we expressed IL-4 in the 4T1^{HUNKsh} by lentiviral transduction (Figure 6a) (shA) & Figure 6b) (shB)). We then isolated CM from these cells and applied it to BMDM from BALB/c *wt* mice or *Il4r*^{-/-} mice. Results show that CM from 4T1^{HUNKsh} cells re-expressing IL-4 rescued pStat6 in *wt* BMDM but did not affect *Il4r*^{-/-} BMDM (Figures 6c,f) (shA), Figures 6d,e) (shB)). Consistent with the IL-4 R blocking antibody experiments shown in Figure 4, loss of IL-4 R in cells isolated from the *Il4r*^{-/-} mice also blocked STAT6 phosphorylation (Figures 6e,f)).

Several studies demonstrated that in breast cancer tumors, IL-4/IL4R is responsible for inducing pro-metastatic growth phenotypes.^{45,46} It has also been shown by Bankaitis and colleagues that a systemic reduction in IL-4 using the 4T1 tumor model limited the burden of metastatic disease in the lungs.⁴³ Therefore, to assess whether IL-4 can rescue metastasis in 4T1^{HUNKsh} tumors we administered IL-4 to mice (Figure 7a)). As previously described, we utilized an orthotopic mammary tumor model and implanted 4T1^{CTL} and the two different 4T1^{HUNKsh} cell lines into the mammary gland of BALB/c female mice. After 1-week post injections, on day 7 we started administration of IL-4 (10ug/kg) treatment which was given to mice every other day for seven more days. On day 15, the experiment was ended, and we analyzed lungs for metastasis. Results show that IL-4 administration does not affect tumor growth (Figure 7b)) but significantly increases lung metastasis, effectively rescuing metastasis in the 4T1^{HUNKsh} groups (Figure 7c,d)). Overall, our findings indicate that HUNK-mediated IL-4 signaling in the tumor microenvironment plays an important role in promoting cancer metastasis.

Discussion

Patient death from TNBC is due to high metastatic rates, relatively poor outcomes, and a lack of sensitivity to endocrine therapy. Therefore, the urgency to identify new biomarkers and target components that help to predict new clinical therapeutics is under high emphasis. In this study, we highlight a new role of HUNK in regulating IL-4 and TAM activation in the TME. Our study establishes the importance of targeting HUNK to modulate TAMs in the TME.

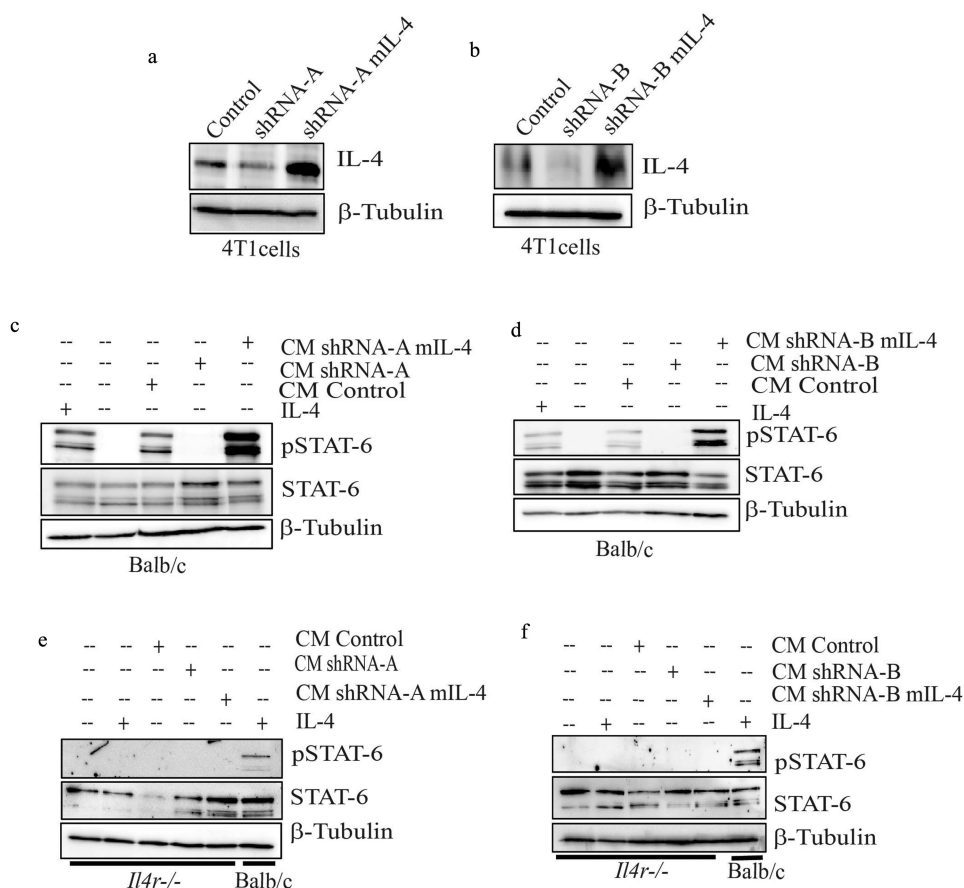


Figure 6. Overexpression of IL-4 in 4T1^{HUNK^{sh}} cells rescues phosphorylation of Stat6. A-B. Western blot analysis showing re-expression of *Il4* in 4T1^{HUNK^{sh}} cells by lentiviral transduction. (shA-panel A, shB-panel B). C-D. BMDM from BALB/c *wt* were treated with condition media (CM) from IL-4 overexpressing 4T1^{HUNK^{sh}} cells (shA-panel C, shB-panel D). CM derived from IL-4 overexpressing 4T1^{HUNK^{sh}} cells resulted in phosphorylation of Stat6 by western blot. BMDM after IL-4 treatment is used as a positive control. E-F. Western blot showing that BMDM from *Il4r*^{-/-} mice treated with CM from IL-4 overexpressing 4T1^{HUNK^{sh}} cells does not result in STAT-6 phosphorylation. The last line to the right represents positive control of BMDM from BALB/c *wt* treated with IL-4.

Cancer cells can modulate and secrete IL-4.^{47,48} In particular, it has been shown that TNBC cells secrete higher levels of IL-4 in the tumor milieu, compared with ER-positive breast cancer cells.⁴⁰ It has also been shown that IL-4 can serve as a key regulator of cancer progression by initiating a paracrine loop between immune cells and tumor cells.¹⁰ The data presented here show that in mouse TNBC cells, HUNK activity regulates the expression and secretion of IL-4. We also show that HUNK regulates IL-4 production in a STAT3-dependent manner. This is consistent with other findings that show STAT3 regulates IL-4 production.³⁴ In particular, STAT3 has been shown to be overexpressed and constitutively activated in TNBC cells, contributing to cancer progression, metastasis, poor survival, and resistance to chemotherapy.^{36,37} Activated STAT3 regulates the expression of different genes involved in cancer cell survival and is also involved in regulating cancer cell immune evasion.³⁶⁻³⁹ In breast cancer cells, it has been shown that STAT3 regulates IL-4 transcription.⁴⁴

Another pathway that has been reported to mediate IL-4 in breast cancer is the EGFR signaling pathway. Liu et al. showed that activation of EGFR results in the expression and secretion of IL-4 in a metastatic breast cancer model.⁴¹ We previously showed that HUNK phosphorylation of EGFR at T654 correlates with increased metastasis in breast cancer *in vivo* tumor studies.²⁵ Therefore, we also tested whether this

phosphorylation would lead to IL-4 regulation. We found that EGFR is not involved in this process. Our results highlight a new signaling pathway by which HUNK kinase activity signals in metastatic breast cancer cells that is independent of EGFR and results in IL-4 production.

IL-4 has been extensively studied in cancer as an important pleiotropic cytokine. IL-4 upregulation and overexpression have been reported to induce pro-tumoral and pro-metastatic functions in different murine and human cancer models.⁴² In the TME, IL-4 activates T_H2 response and TAMs.⁴⁹ In breast cancer, it is reported that IL-4 can differentiate macrophages into an M2-like TAM phenotype, enhancing the invasion and migration of breast cancer cells.⁵⁰ Our data confirmed what others reported, that metastatic breast cancer cells, here we use the 4T1 cell line, express and secrete IL-4. Secreted IL-4 then induces polarization of macrophages into an M2-like TAM phenotype. Our new data show that HUNK regulates IL-4 production and that the depletion of HUNK impairs this effect. We also show that M2-like activation in our model is primarily regulated by the IL-4 receptor signaling pathway on macrophages. Our studies show that IL-4 secreted from tumor cells activates IL-4 R on macrophages leading to activation of Stat6. There is evidence of a multifunctional role of IL-4 as an important regulator of other immune cells, including activation of CD8⁺ T cells.⁴⁹ Our study does not explore the

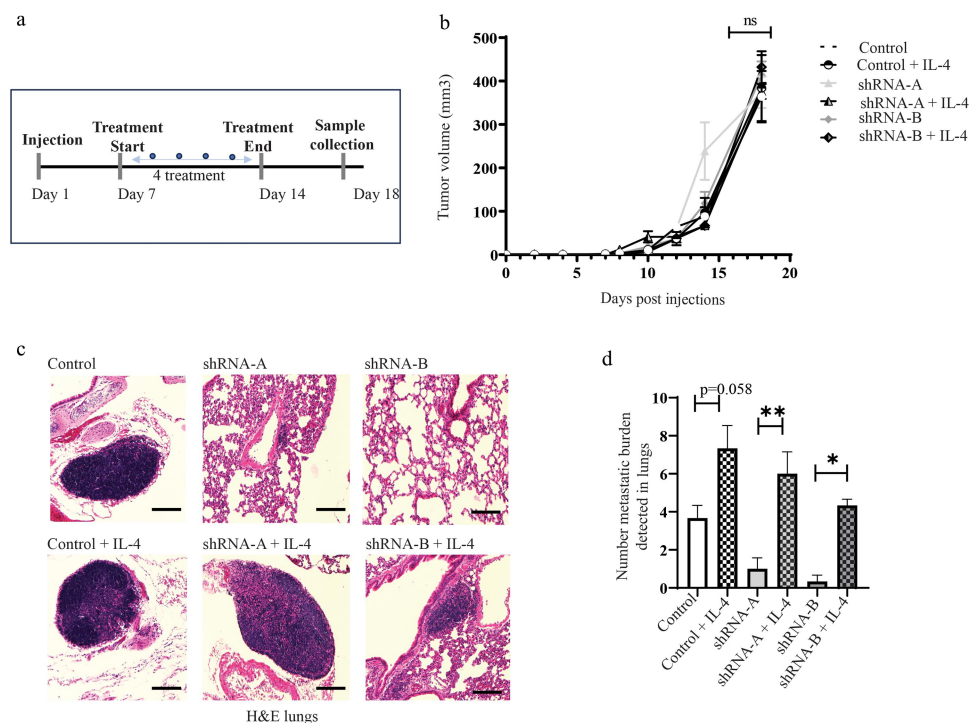


Figure 7. Metastasis is rescued in mice with 4T1^{HUNKsh} tumors by IL-4 administration. A. Schematic representation of IL-4 treatment. After 1-week post-injection, mice were i.p. treated with vehicle (PBS) or recombinant IL-4 (10 ug/kg) every other day for 1 week. After the end of treatment (on day 14) mice were placed under observation for 5 d; samples were collected on day 18. Tumors and lungs derived from 4T1^{CTL} and 4T1^{HUNKsh} orthotopic models with or without IL-4 treatment were analyzed for tumor growth (B) and metastasizes by H&E staining (100 mm scale bar) (C-D). $N \geq 3$ mice per group. Statistical analyses were performed using one-way and two-way ANOVA. Data are expressed as mean \pm SEM. *, $p < 0.05$; **, $p < 0.01$.

activation of T-cells, but this does not exclude the fact that this could also occur in our system. It has also been reported that IL-4 induces metastatic growth phenotypes in breast cancer.⁴⁵ Prior evidence has shown that up-regulation of IL-4/IL-4 R signaling is associated with poor prognosis in both human and murine models, and IL-4 inhibition significantly reduces invasion to distant sites of breast cancer cells.^{45,51,52} Our data show that exogenously delivered IL-4 into mice promoted metastasis. Lungs from mice with 4T1^{HUNKsh} tumors that were administered IL-4 had significantly increased lung metastasis when compared to the placebo group. Contrary to others who have reported that in breast cancer IL-4 stimulates tumor growth,⁵³ our data fail to replicate those results. This could be due to the source of IL-4 or the amount of time that mice were exposed to IL-4. There is a correlation between the role that IL-4 plays in tumor immunity and cancer tumorigenesis. Endogenous IL-4 has been found to promote tumor growth, while exogenously delivered IL-4 is often linked to tumor growth suppression.⁵⁴ Indeed, we elected to use recombinant IL-4 for our studies because the amount of IL-4 generated from the 4T1^{HUNKsh} cells that we engineered to stably express mLIL-4 was quite high and providing recombinant IL-4 allowed us to more carefully control the *in vivo* analysis. Future studies could be geared toward exploring the effects of endogenous IL-4.

TAMs can promote tumor growth by secreting growth factors that induce angiogenesis and support EMT.^{10,15,35} In particular, TAMs overexpress EGF, which is associated with metastasis.^{39,55} Seminal work from Wyckoff et al. showed that an EGF-dependent paracrine loop between tumor cells

and macrophages is required for mammary tumor cell migration.³⁸ In the TME macrophages will produce EGF, where cancer cells expressing EGF receptors will get activated by EGF, which subsequently promotes migration of the cancer cells in a codependent manner with the TAMs.^{38,39,56} Furthermore, results from Goswami, et al. also showed in a co-culture-based *in vitro* model of macrophages and breast cancer cells that EGF expressed by macrophages but not cancer cells is required to promote cell invasion.³⁹

Intriguingly, our data show that TAMs isolated from 4T1^{CTL}-derived tumors express high levels of EGF and that tumors derived from 4T1 cells after depletion of HUNK lead to a loss of IL-4 secretion and suppress EGF production from TAMs isolated from the 4T1^{HUNKsh} tumors. This finding correlates with higher metastasis levels we see in tumors derived from 4T1^{CTL} cells compared to those derived from 4T1^{HUNKsh} cells. Our data demonstrate that a paracrine loop exists between macrophages and tumor cells in the mammary tumor TME that is controlled by HUNK. HUNK causes secretion of IL-4 from tumor cells, leading to the activation of IL-4 R on TAMs that in turn produce EGF. EGF then signals back to EGFR on the tumor cells. Our prior work further shows that HUNK phosphorylates EGFR to promote metastatic signaling and metastasis of tumor cells.²⁴ Our findings are significant because they implicate HUNK as a multi-functional metastatic target in the tumor cell that can impact the bidirectional nature of the paracrine signaling loop to TAMs which is critical for metastasis (Supplementary Figure S6). Importantly, our data

highlight the potential of targeting HUNK as a novel treatment of TNBC and HUNK's promising role as a key immune regulator of M2-like TAMs.

Acknowledgments

This work was supported by funding agency National Cancer Institute (NCI) grant number RO3 CA187305 and RO1 CA269508 to ESY. This project was also supported by grants from the IU Simon Comprehensive Cancer Center and the 100 Voices of Hope and supported by the Brown Center for Immunotherapy (MHK). AC was supported by the funding agency National Institutes of Health (NIH) grant number T32 HL007910. NRS was supported by funding agency National Institutes of Health (NIH) grant number T32 AI060519. The authors would also like to acknowledge Dr. Xiongbin Lu for kindly sharing the EO771 cell line as an experimental model utilized in the work.

Disclosure statement

No potential conflict of interest was reported by the author(s).

Funding

The work was supported by the National Cancer Institute [RO3 CA187305]; National Cancer Institute [RO1 CA269508]; National Heart, Lung, and Blood Institute [T32 HL007910]; National Institute of Allergy and Infectious Diseases [T32 AI060519]; IU Simon Comprehensive Cancer Center 100 Voices of Hope and supported by the Brown Center for Immunotherapy.

Author contributions

NRS conceived the experimental design and work presented in the study, retrieved the relevant literature, and completed the writing of the manuscript, including preparing figures, statistical analysis, and tables. AC prepared a flow cytometry panel and ran the instrument. TD and MA played a part in tumor monitoring and isolation. AO performed gene expression analysis using NanoString's nCounter PanCancer Immune Profiling panel. ESY oversaw the design and execution of all studies, revised, edited, and contributed intellectually to the preparation of the manuscript. MK and AS provided intellectual knowledge and expertise in the analysis of TAMs and flow cytometry. All authors have read and agreed to the published version of the manuscript.

Data availability statement

Data for NanoString's nCounter PanCancer Immune Profiling panel can be accessed via NCBI GEO (GSE242859 study).

References

- Bou Zerdan M, Ghorayeb T, Saliba F, Allam S, Bou Zerdan M, Yaghi M, Bilani N, Jaafar R, Nahleh Z. Triple negative breast cancer: updates on classification and treatment in 2021. *Cancers (Basel)*. 2022;14(5). doi:10.3390/cancers14051253.
- Kenakin TP, Kenakin TP. *Comprehensive pharmacology*. Amsterdam (Netherlands): Elsevier; 2022.
- Yeh NR-SAE. Triple negative breast cancer. In: Kenakin T, editor. *Comprehensive pharmacology*. London (UK): Elsevier; 2022. p. 35–48.
- Draganescu M and Carmocan C. Hormone therapy in breast cancer. *Chirurgia (Bucur)*. 2017;112(4):413–417. doi:10.21614/chirurgia.112.4.413.
- Dietze EC, Sistrunk C, Miranda-Carboni G, O'Regan R, Seewaldt VL. Triple-negative breast cancer in African-American women: disparities versus biology. *Nat Rev Cancer*. 2015;15(4):248–254. doi:10.1038/nrc3896.
- Fan Y, He S. The characteristics of tumor microenvironment in triple negative breast cancer. *Cancer Manag Res*. 2022;14:1–17. doi:10.2147/CMAR.S316700.
- Yu T, Di G. Role of tumor microenvironment in triple-negative breast cancer and its prognostic significance. *Chinese J Cancer Res*. 2017;29(3):237–252. doi:10.21147/j.issn.1000-9604.2017.03.10.
- Yin L, Duan JJ, Bian XW, Yu SC. Triple-negative breast cancer molecular subtyping and treatment progress. *Breast Cancer Res*. 2020;22(1):61. doi:10.1186/s13058-020-01296-5.
- Stanton SE, Disis ML. Clinical significance of tumor-infiltrating lymphocytes in breast cancer. *J Immunother Cancer*. 2016;4(1):59. doi:10.1186/s40425-016-0165-6.
- Kitano A, Ono M, Yoshida M, Noguchi E, Shimomura A, Shimoi T, Kodaira M, Yunokawa M, Yonemori K, Shimizu C, et al. Tumour-infiltrating lymphocytes are correlated with higher expression levels of PD-1 and PD-L1 in early breast cancer. *ESMO Open*. 2017;2(2):e000150. doi:10.1136/esmoopen-2016-000150.
- Zhang WJ, Wang XH, Gao ST, Chen C, Xu XY, Sun Q, Zhou Z-H, Wu GZ, Yu Q, Xu G, et al. Tumor-associated macrophages correlate with phenomenon of epithelial-mesenchymal transition and contribute to poor prognosis in triple-negative breast cancer patients. *J Surg Res*. 2018;222:93–101. doi:10.1016/j.jss.2017.09.035.
- Yuan ZY, Luo R-Z, Peng R-J, Wang S-S, Xue C. High infiltration of tumor-associated macrophages in triple-negative breast cancer is associated with a higher risk of distant metastasis. *Onco Targets Ther*. 2014;7:1475–1480. doi:10.2147/OTT.S61838.
- Shinohara H, Kobayashi M, Hayashi K, Nogawa D, Asakawa A, Ohata Y, Kubota K, Takahashi H, Yamada M, Tokunaga M, et al. Spatial and quantitative analysis of tumor-associated macrophages: intratumoral CD163-/PD-L1+ TAMs as a marker of favorable clinical outcomes in triple-negative breast cancer. *Int J Mol Sci*. 2022;23(21):23. doi:10.3390/ijms232113235.
- Yang J, Liao D, Chen C, Liu Y, Chuang T-H, Xiang R, Markowitz D, Reisfeld RA, Luo Y. Tumor-associated macrophages regulate murine breast cancer stem cells through a novel paracrine EGFR/Stat3/Sox-2 signaling pathway. *Stem Cells*. 2013;31(2):248–258. doi:10.1002/stem.1281.
- Noy R, Pollard JW. Tumor-associated macrophages: from mechanisms to therapy. *Immunity*. 2014;41(1):49–61. doi:10.1016/j.immuni.2014.06.010.
- Jayasingam SD, Citartan M, Thang TH, Mat Zin AA, Ang KC, Ch'ng ES. Evaluating the polarization of tumor-associated macrophages into M1 and M2 phenotypes in human cancer tissue: Technicalities and challenges in routine clinical practice. *Front Oncol*. 2020;9:1512. doi:10.3389/fonc.2019.01512.
- Pan Y, Yu Y, Wang X, Zhang T. Tumor-associated macrophages in tumor immunity. *Front Immunol*. 2020;11:583084. doi:10.3389/fimmu.2020.583084.
- Williams CB, Yeh ES, Soloff AC. Tumor-associated macrophages: unwitting accomplices in breast cancer malignancy. *NPJ Breast Cancer*. 2016;2(1):15025–. doi:10.1038/npjbcancer.2015.25.
- Boutillier AJ, ElSawa SF. Macrophage polarization states in the tumor microenvironment. *Int J Mol Sci*. 2021;22(13):6995. doi:10.3390/ijms22136995.
- Yang L, Zhang Y. Tumor-associated macrophages: from basic research to clinical application. *J Hematol Oncol*. 2017;10(1):58. doi:10.1186/s13045-017-0430-2.
- Gordon S. Alternative activation of macrophages. *Nat Rev Immunol*. 2003;3(1):23–35. doi:10.1038/nri978.
- Wertheim GB, Yang TW, Pan T-C, Ramne A, Liu Z, Gardner HP, Dugan KD, Kristel P, Kreike B, van de Vijver MJ, et al. The Snf1-related kinase, hunk, is essential for mammary tumor metastasis. *Proc Natl Acad Sci USA*. 2009;106(37):15855–15860. doi:10.1073/pnas.0906993106.
- Yeh ES, Abt MA, Hill EG. Regulation of cell survival by HUNK mediates breast cancer resistance to HER2 inhibitors. *Breast*

- Cancer Res Treat. 2015;149(1):91–98. doi:10.1007/s10549-014-3227-9.
24. Yeh ES, Yang TW, Jung JJ, Gardner HP, Cardiff RD, Chodosh LA. Hunk is required for HER2/neu-induced mammary tumorigenesis. *J Clin Invest*. 2011;121(3):866–879. doi:10.1172/JCI42928.
 25. Williams CB, Phelps-Polirer K, Dingle IP, Williams CJ, Rhett MJ, Eblen ST, Armeson K, Hill EG, Yeh ES. HUNK phosphorylates EGFR to regulate breast cancer metastasis. *Oncogene*. 2020;39(5):1112–1124. doi:10.1038/s41388-019-1046-5.
 26. Chodosh LA, Gardner HP, Rajan JV, Stairs DB, Marquis ST, Leder PA. Protein kinase expression during murine mammary development. *Dev Biol*. 2000;219(2):259–276. doi:10.1006/dbio.2000.9614.
 27. Ramos-Solis N, Dilday T, Kritikos AE, Yeh ES. HUNK gene alterations in breast cancer. *Biomedicines*. 2022;10(12):10. doi:10.3390/biomedicines10123072.
 28. Zhong Z, Wen Z, Darnell JE. Stat3 and Stat4: members of the family of signal transducers and activators of transcription. *Proc Natl Acad Sci USA*. 1994;91(11):4806–4810. doi:10.1073/pnas.91.11.4806.
 29. Pineda-Torra I, Gage M, de Juan A, Pello OM. Isolation, culture, and polarization of murine bone marrow-derived and peritoneal macrophages. *Methods Mol Biol*. 2015;1339:101–109.
 30. Burgess AW. EGFR family: structure physiology signalling and therapeutic targets †. *Growth Fact*. 2008;26(5):263–274. doi:10.1080/08977190802312844.
 31. Ettenberg SA, Keane MM, Nau MM, Frankel M, Wang L-M, Pierce JH, Lipkowitz S. cbl-b inhibits epidermal growth factor receptor signaling. *Oncogene*. 1999;18(10):1855–1866. doi:10.1038/sj.onc.1202499.
 32. So EY, Oh J, Jang J-Y, Kim J-H, Lee C-E. Ras/Erk pathway positively regulates Jak1/STAT6 activity and IL-4 gene expression in Jurkat T cells. *Mol Immunol*. 2007;44(13):3416–3426. doi:10.1016/j.molimm.2007.02.022.
 33. Jorritsma PJ, Brogdon JL, Bottomly K. Role of TCR-induced extracellular signal-regulated kinase activation in the regulation of early IL-4 expression in naive CD4+ T cells. *J Immunol*. 2003;170(5):2427–2434. doi:10.4049/jimmunol.170.5.2427.
 34. Sun Y, Dong Y, Liu X, Zhang Y, Bai H, Duan J, Tian Z, Yan X, Wang J, Wang Z, et al. Blockade of STAT3/IL-4 overcomes EGFR T790M-cis-L792F-induced resistance to osimertinib via suppressing M2 macrophages polarization. *EBioMedicine*. 2022;83:104200. doi:10.1016/j.ebiom.2022.104200.
 35. Wang HW, Joyce JA. Alternative activation of tumor-associated macrophages by IL-4: priming for protumoral functions. *Cell Cycle*. 2010;9(24):4824–4835. doi:10.4161/cc.9.24.14322.
 36. de Groot AE, Myers KV, Krueger TEG, Brennen WN, Amend SR, Pienta KJ. Targeting interleukin 4 receptor alpha on tumor-associated macrophages reduces the pro-tumor macrophage phenotype. *Neoplasia*. 2022;32:100830. doi:10.1016/j.neo.2022.100830.
 37. Li Y, Sheng Q, Zhang C, Han C, Bai H, Lai P, Fan Y, Ding Y, Dou X. STAT6 up-regulation amplifies M2 macrophage anti-inflammatory capacity through mesenchymal stem cells. *Int Immunopharmacol*. 2021;91:107266. doi:10.1016/j.intimp.2020.107266.
 38. Wyckoff J, Wang W, Lin EY, Wang Y, Pixley F, Stanley ER, Graf T, Pollard JW, Segall J, Condeelis J, et al. A paracrine loop between tumor cells and macrophages is required for tumor cell migration in mammary tumors. *Cancer Res*. 2004;64(19):7022–7029. doi:10.1158/0008-5472.CAN-04-1449.
 39. Goswami S, Sahai E, Wyckoff JB, Cammer M, Cox D, Pixley FJ, Stanley ER, Segall JE, Condeelis JS. Macrophages promote the invasion of breast carcinoma cells via a colony-stimulating factor-1/Epidermal growth factor paracrine loop. *Cancer Res*. 2005;65(12):5278–5283. doi:10.1158/0008-5472.CAN-04-1853.
 40. Gaggianesi M, Turdo A, Chinnici A, Lipari E, Apuzzo T, Benfante A, Sperduti I, Di Franco S, Meraviglia S, Lo Presti E, et al. IL4 primes the dynamics of breast cancer progression via DUSP4 inhibition. *Cancer Res*. 2017;77(12):3268–3279. doi:10.1158/0008-5472.CAN-16-3126.
 41. Liu H-T, Gao ZX, Guo XY, Zhou XC, Zhao RN, Liu S, Zhu WJ, Zhang FZ, Wang H, Zhao CZ. THAP7-AS1 recruits the SWI/SNF to activate EGFR-ELK1 signaling and induce crosstalk between tumor-associated macrophages and breast cancer cells. *Research Square*; 2022.
 42. Suzuki A, Leland P, Joshi BH, Puri RK. Targeting of IL-4 and IL-13 receptors for cancer therapy. *Cytokine*. 2015;75(1):79–88. doi:10.1016/j.cyto.2015.05.026.
 43. Bankaitis KV, Fingleton B. Targeting IL4/IL4R for the treatment of epithelial cancer metastasis. *Clin Exp Metastasis*. 2015;32(8):847–856. doi:10.1007/s10585-015-9747-9.
 44. Noben-Trauth N, Shultz LD, Brombacher F, Urban JF, Gu H, Paul WE. An interleukin 4 (IL-4)-independent pathway for CD4 + T cell IL-4 production is revealed in IL-4 receptor-deficient mice. *Proc Natl Acad Sci USA*. 1997;94(20):10838–10843. doi:10.1073/pnas.94.20.10838.
 45. Venmar KT, Carter KJ, Hwang DG, Dozier EA, Fingleton B. IL4 receptor ILR4a regulates metastatic colonization by mammary tumors through multiple signaling pathways. *Cancer Res*. 2014;74(16):4329–4340. doi:10.1158/0008-5472.CAN-14-0093.
 46. Hallett MA, Venmar KT, Fingleton B. Cytokine stimulation of epithelial cancer cells: the similar and divergent functions of IL-4 and IL-13. *Cancer Res*. 2012;72(24):6338–6343. doi:10.1158/0008-5472.CAN-12-3544.
 47. Zheng Y, Ren S, Zhang Y, Liu S, Meng L, Liu F, Gu L, Ai N, Sang M. Circular RNA circWWC3 augments breast cancer progression through promoting M2 macrophage polarization and tumor immune escape via regulating the expression and secretion of IL-4. *Cancer Cell Int*. 2022;22(1):264. doi:10.1186/s12935-022-02686-9.
 48. Lin X, Wang S, Sun M, Zhang C, Wei C, Yang C, Dou R, Liu Q, Xiong B. Retracted article: miR-195-5p/NOTCH2-mediated EMT modulates IL-4 secretion in colorectal cancer to affect M2-like TAM polarization. *J Hematol Oncol*. 2019;12(1):20. doi:10.1186/s13045-019-0708-7.
 49. DeNardo DG, Barreto JB, Andreu P, Vasquez L, Tawfik D, Kolhatkar N, Coussens LM. CD4+ T cells regulate pulmonary metastasis of mammary carcinomas by enhancing protumor properties of macrophages. *Cancer Cell*. 2009;16(2):91–102. doi:10.1016/j.ccr.2009.06.018.
 50. Little AC, Pathanjeli P, Wu Z, Bao L, Goo LE, Yates JA, Oliver CR, Soellner MB, Merajver SD. IL-4/IL-13 stimulated macrophages enhance breast cancer invasion via Rho-GTPase regulation of synergistic VEGF/CCL-18 signaling. *Front Oncol*. 2019;9:456. doi:10.3389/fonc.2019.00456.
 51. König A, Vilsmaier T, Rack B, Friese K, Janni W, Jeschke U, Andergassen U, Trapp E, Jückstock J, Jäger B, et al. Determination of Interleukin-4, -5, -6, -8 and -13 in serum of patients with breast cancer before treatment and its correlation to circulating tumor cells. *Anticancer Res*. 2016;36(6):3123–3130.
 52. Parveen S, Siddharth S, Cheung LS, Kumar A, Shen J, Murphy JR, Sharma D, Bishai WR. Therapeutic targeting with DABIL-4 depletes myeloid suppressor cells in 4T1 triple-negative breast cancer model. *Mol Oncol*. 2021;15(5):1330–1344. doi:10.1002/1878-0261.12938.
 53. Venmar KT, Kimmel DW, Cliffl DE, Fingleton B. IL4 receptor a mediates enhanced glucose and glutamine metabolism to support breast cancer growth. *Biochim Biophys Acta*. 2015;1853(5):1219–1228. doi:10.1016/j.bbamer.2015.02.020.
 54. Li Z, Chen L, Qin Z. Paradoxical roles of IL-4 in tumor immunity. *Cell Mol Immunol*. 2009;6(6):415–422. doi:10.1038/cmi.2009.53.
 55. Leek RD, Hunt NC, Landers RJ, Lewis CE, Royds JA, Harris AL. Macrophage infiltration is associated with VEGF and EGFR expression in breast cancer. *J Pathol*. 2000;190(4):430–436. doi:10.1002/(SICI)1096-9896(200003)190:4<430::AID-PATH538>3.0.CO;2-6.
 56. Lin EY, Nguyen AV, Russell RG, Pollard JW. Colony-stimulating factor 1 promotes progression of mammary tumors to malignancy. *J Exp Med*. 2001;193(6):727–740. doi:10.1084/jem.193.6.727.